Available online at www.sciencedirect.com
SCIENCE DIRECT®
ELSEVIER
Nuclear Instruments and Methods in Physics Research B 234 (2005) 431–440
NIM B
Beam Interactions with Materials & Atoms
www.elsevier.com/locate/nimb

Experimental investigation of the ionization dynamics in slow p–H_2 collisions

F. Afaneh [a,*], R. Dörner [b], L.Ph.H. Schmidt [b], H. Schmidt-Böcking [b]

[a] *Department of Physics, The Hashemite University, P.O. Box 150459, Zarqa 13115, Jordan*
[b] *Institut für Kernphysik, August-Euler-Straße 6, 60486 Frankfurt am Main, Germany*

Received 24 October 2004; received in revised form 6 February 2005
Available online 2 June 2005

Abstract

The single ionization (SI) and the transfer ionization (TI) of H_2 have been investigated utilizing the Cold Target Recoil Ion Momentum Spectroscopy (COLTRIMS) reaction microscope. Continuum electron velocity spectra have been measured for experimentally determined nuclear motion. Electron velocity distributions for the SI of H_2 show that the ejected electrons lie mainly in the scattering plane where their velocities were found to lie between those of the recoiling target and the scattered projectile. In addition to a group of electrons seen in SI saddle electrons group, the electron velocity spectra for TI of H_2 unveiled the existence of another group of electrons with different structure. These electrons were emitted with velocities greater than the projectile velocity and found to result from a narrow range of impact parameters. These fast forward electrons reveal a substantial amount of out-of-plane scattering.

PACS: 34.50.Gb; 34.70.+e; 39.30.+w

1. Introduction

A major problem in molecular physics is ionization in ion–molecule collisions. The continuum distribution of electrons ejected in such collisions is still not completely understood particularly at impact velocities where the collision dynamics possess a molecular character. In slow collisions the electronic wavefunction has time to adjust adiabatically to the slowly changing two-center potential of the target and projectile forming an intermediate quasi-molecule. On rupture of this quasi-molecule the electrons relax in most cases into bound states of either the target or the projectile. In a few cases, however, one electron is promoted to the continuum, leading to ionization.

* Corresponding author. Present address: P.O. Box 330039, Zarqa 13133, Jordan. Tel.: +962 795576035; fax: +962 5 3826613.
E-mail addresses: afaneh@hu.edu.jo, afaneh@hsb.uni-frankfurt.de (F. Afaneh).

0168-583X/$ - see front matter
doi:10.1016/j.nimb.2005.02.028

The mechanisms leading to this ejection of electrons are still controversial. On the theoretical side, one of the most surprising theoretical predictions has been the existence of the so-called ''saddle-point ionization mechanism''. Saddle point electrons were found in classical trajectory Monte Carlo (CTMC) calculations [1–3] and also in triple center close-coupling calculations [4,5] demonstrating the possibility of electrons being balanced by the attractive Coulomb forces of the two nuclei, in a way being ''stranded in'' between the nuclei on the saddle point (top of the internuclear potential barrier). When an electron stays localized near this point until the completion of the collisional interaction, the electron will no longer be bound to nuclei and so ionization takes place. In order to examine the importance of the potential saddle in ionization, Bandarage and Parson [6] have carried out an analysis of the evolution of the electron's energy as the two nuclei separate by defining an electron's energy with respect to a moving molecular frame. Their results supported the existence of the saddle point electrons. From a study of the separate time evolutions of molecular-type and nonmolecular ionizing distributions for He^{2+} + H(1s) collisions, Illescas et al. [7] concluded that ''at sufficiently low nuclear velocities, the ionization mechanism is determined by the molecular-type distributions and also at these velocities, this mechanism may also be properly qualified as saddle-point ionization''. In quantum mechanical calculations employing the semiclassical approximation, Ovchinnikov et al. [8] have developed an approach known later as Hidden Crossing Theory, which enabled them to explain the saddle point electrons. The method is based on the analytical continuation of adiabatic potential energy curves in the complex plane of the internuclear distance. In this plane the energy states with the same symmetry are connected by branch points. Using phase integrals around these points, Pieksma et al. [9] have determined the ionization cross sections for H^+ + H collisions. These calculations of the total cross sections have identified two ionization mechanisms. One is related to the saddle point called T *series*. A second mechanism occurs at rather small internuclear distances called S *series*. While the S *series* indicates the region where the united atom approximation breaks down, the T series determines the region where the system has quasi-molecular structure. In T mechanism, two series of transitions, the T00 and T01, were found to contribute to the saddle point mechanism. In a further extension, the Sturmian theory was developed with the aim of providing a full description of the ionization process, including the prediction of the velocity distribution of the ejected electron. Applying Sturmian theory to the H^+ + H collisions, the T00 promotion of the 1sσ and the T01 promotion of the 2pπ states were carried out [10,11]. The electron velocity distribution obtained from the T00 promotion gives a single peak centered on the potential saddle (σ orbitals) and T01 promotion predicts the double-peak structure in the transverse direction, as one expects from π orbitals. To obtain the complete velocity distribution of the electron near the saddle point, it was assumed that the T00 and T01 are the main contributors of saddle-point electrons. The phase between the two paths to ionization was calculated by Macek et al. [12], showing a strong dependence on projectile velocity, and thus the two peaks in the transverse velocity distribution exhibit rapid oscillations with collision energy. This behavior has also been seen by Dörner et al. [13] in their experimental study of electron ejection in the H^+ + He collisions for low impact energies (5–15 keV) using COLTRIMS technique. More recently, solutions of the time-dependent Schrödinger equation illustrated the details of the complicated evolution of the electron cloud finally leading to continuum electrons [14,15]. The CTMC investigation of the role of the saddle point promotion in the slow collisions presented in [3] has suggested that only a small fraction of the continuum electrons released in p on H collisions at 1 a.u. velocity originates from the saddle point ionization mechanism. This result does not agree with the conclusions drawn from the hidden crossing theory [11,12]. The relationships between these rivaling theoretical approaches remain to be clarified.

On the experimental side, with the development of the COLTRIMS technique [16,17], the experimental study of electron emission in slow ion–atom and ion–molecule collisions has received a fresh input. These experiments have succeeded to provide a first detailed view of the velocity

distributions of continuum electrons [18–23]. These experimental images of the velocity distribution of continuum electrons obtained in these experiments unveiled a rich structure in the saddle region between the target and projectile velocity. Using the COLTRIMS technique, Kravis et al. [18] measured for the first time the two- dimensional velocity distribution of the emitted electrons in ionization of He by protons and bare carbon nuclei at a wide range of impact velocities. They were however unable to determine the impact parameter. Only for the case of proton impact below 1 a.u., they found that most of the ejected electrons lie in the saddle point region. The discussion of the saddle ionization mechanism has been profoundly changed through the experimental work of Dörner et al. [13]. They utilized the COLTRIMS technique in studying electron emission in the p–He collisions for low impact energies (5, 10 and 15 keV) and used the momentum of the recoil ion to select the scattering plane and impact parameter. They found that electrons were ejected within the scattering plane and into the forward direction. The in-scattering velocity distributions showed a two-finger structure, one finger extending away from the projectile direction and the other toward it. These features, as mentioned above, were first interpreted by Ovchinnikov and Macek [10,11] who attributed the origin of this oscillation to interference between σ and π amplitudes in the continuum, with a relative phase, which varied inversely with the projectile velocity. With a similar COLTRIMS setup as the one used by Dörner et al., further experimental studies have been carried out by Abdallah et al. [19–21], Afaneh et al. [22], and Schmidt et al. [23] to study ionization in collisions of He^+, He^{2+} and Ne^+ with He, H_2 and Ne. These experiments revealed striking patterns in the velocity distributions of the emitted electrons. These patterns were interpreted as the structure of the molecular orbitals whose promotion into the continuum was responsible for the ionization.

In this paper we report on the experimental study of ionization processes in 15 keV p–H_2 collisions utilizing the COLTRIMS reaction microscope. The single ionization (SI) of H_2

$$p + H_2 \rightarrow p + H_2^+ + e^- \quad (1)$$

which leads to H_2^+ recoil ions in nondissociative states as well as the transfer ionization (TI) of H_2

$$p + H_2 \rightarrow H + H^+ + H^+ + e^- \quad (2)$$

which leads to H_2 dissociation into two free protons, have been investigated. Velocity spectra of continuum electrons have been measured for experimentally determined nucl7ear motion, i.e. the three-dimensional momentum vector of the recoil ion H_2^+ in reaction (1) or the momentum vectors of both fragments in reaction (2).

2. Experimental setup

The experiment was carried out at the Electron Cyclotron Resonance Ion Source (ECRIS) installed in the Institute of Nuclear Physics at Frankfurt University using Cold Target Recoil Ion Momentum Spectroscopy (COLTRIMS) [16,17,22]. Fig. 1 illustrates the experimental setup. The well-collimated ion beam (z-axis) crossed a well-localized and internally cold gas target (y-axis) provided by a two-stage supersonic gas jet. An electric field (x-axis) of 13 V/mm perpendicular to both the ion beam and the gas jet was used to extract the recoil ions and slow ejected electrons in opposite directions. Electrons were accelerated by this field for a distance of 15 mm, then drifted a distance of 40 mm to be detected by a position-sensitive detector. A small negative bias voltage was applied to the first channel plate of this detector to repel background electrons. The recoil ions were accelerated in the opposite direction over a distance of 35 mm and subsequently traversed a field-free region of 128 mm to be detected by a multi-hit position-sensitive detector. The extraction field was shaped slightly so as to focus a parallel beam from the interaction region onto the recoil detector and was arranged also to provide first-order time focusing for the recoil ions. The time-of-flight of the electron was about 11 ns and had a small spread of only about 2.5 ns. This allowed us to use the electron time signal as a start for the time-to-amplitude converter, which was stopped by the recoil time signal. The measured time-of-flight of recoil ion was used in calculating one of the momentum components of the recoil ions. The other two components were

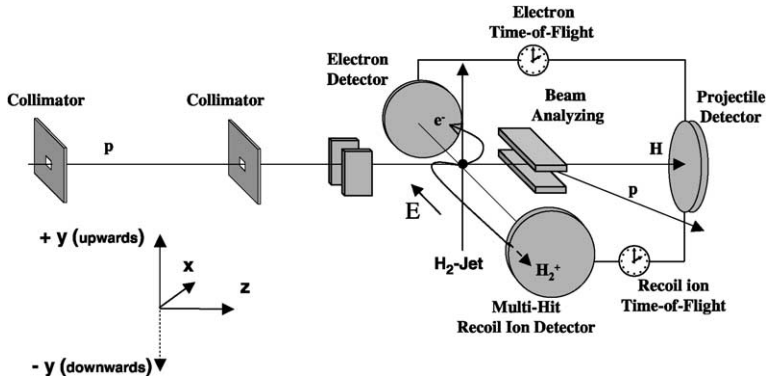

Fig. 1. Schematic diagram of the experimental setup.

calculated from the position on the detector. Two of the three velocity components of the electrons were calculated from the electron position on the electron detector assuming a constant time-of-flight. The outgoing projectile ions were charge state analyzed and detected by a third position-sensitive detector located 3.5 m downstream. The main beam was prevented from reaching the projectile detector due to the high intensity of the beam. It was deflected after penetrating the target and dumped into a Faraday cup.

3. Results and discussion

For a convenient presentation of the results, two-dimensional ($V_{e,z}$, $V_{e,y}$) velocity distributions of the emitted electrons were generated for different conditions on the direction of the recoil ions. Two particular electron velocity distributions are of interest: one for which the recoil-ion momenta are required to lie parallel to the plane of the electron detector, the yz-plane (see Fig. 1), which yields a "top view" of the emitted electrons, looking down on the nuclear scattering plane, and one for which the recoil momenta are required to be along the x-axis, which yields a "side view" of the ejected electrons, looking edge-on along the collision plane. In all top-view figures, the recoil is directed downwards, i.e. the projectile was scattered upwards. Electron velocities are measured in units of the projectile velocity V_p. Target-centered electron emission appears around the origin ($V_{e,z} = 0$ and $V_{e,y} = 0$) while electrons captured to continuum states of the projectile are located at ($V_{e,z}/V_p = 1$ and $V_{e,y} = 0$). Electrons from the saddle point are located near the center between target and projectile, saddle electrons.

Fig. 2(a) and (b) show the side and top views of the ejected electron velocity distribution in the collision 15 keV p^+ on H_2 leading to the single ionization of H_2 (reaction 1). The figures display that most electrons liberated during the collision lie mainly in the scattering plane. This can be understood as a consequence of linear momentum conservation. Longitudinal velocity distribution ($V_{e,z}$) of the ejected electrons for the side and top views are given in Fig. 3(a). This figure show that the longitudinal velocities of these electrons were found to lie between those of the target and the projectile, i.e. in the vicinity of the saddle point. The top-view of the electron velocity distribution in Fig. 2(b) has a maximum at the internuclear axis. This suggests that the contribution of the σ orbital in the ionization process is dominant, leading to the concentration of the electrons around the internuclear axis. This structure can be seen more clearly by making a transverse projection of a slice of the two-dimensional distribution near $V_{e,z}/V_p = 0.5$. Such a projection of Fig. 2(b) is shown in Fig. 3(b). The dependence of these patterns observed in the in-scattering velocity distribution on the transverse momentum transfer to the recoil is also studied. This momentum is approximately a measure of the impact parameter, since the transverse momentum transfer to the

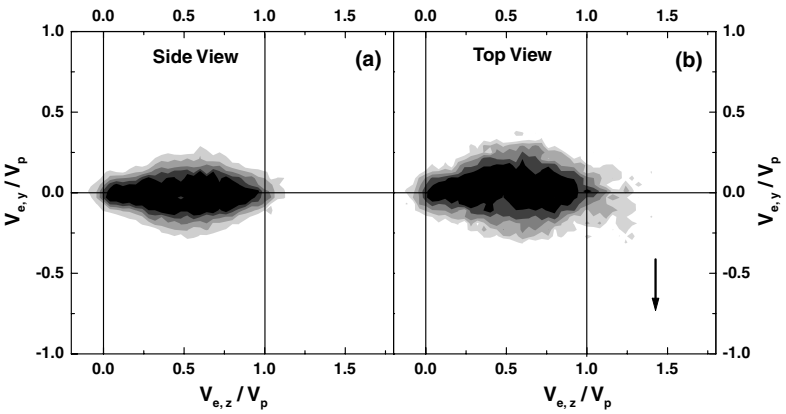

Fig. 2. (a) Side view and (b) top view of the ejected electron velocity distribution in the collision $V_p = 0.78$ a.u. p on H_2 leading to H_2^+ recoil ions in nondissociative states ($p + H_2 \rightarrow p + H_2^+ + e^-$). The intensity of each cell is proportional to the number of counts in that cell. Each image has been normalized so its maximum intensity is near ten units on this scale. The electron velocity components $V_{e,y}$ and $V_{e,z}$ are scaled by the projectile velocity.

Fig. 3. (a) The Z-component of the velocity of electrons ejected in the collision $V_p = 0.78$ a.u. p on H_2 leading to the single ionization of H_2. (b) Vertical slices from (a) and (b) projected onto the $V_{e,y}/V_p$ axis for $0.4 < V_{e,z}/V_p < 0.6$.

electron is small. The electron velocity distribution was generated for different windows on the magnitude of the recoil-ion transverse momentum. The results are shown in Fig. 4. In these figures the recoil-ion transverse momentum increases in moving from Fig. 4(a)–(d). The corresponding transverse projections of slices from each distribution near $V_{e,z}/V_p = 0.5$ are given in Fig. 4(e)–(h). The figures show that the distribution exhibits a maximum at the internuclear axis (σ structure) for small recoil-ion transverse momenta (distant collisions) and a nodal line along the internuclear axis (π structure) for large recoil-ion transverse momenta (close collisions). The structures observed in these velocity distributions are in agreement with the explanation of the saddle point ionization mechanism suggested by Ovchinnikov et al. [10,11] and Macek et al. [12] within the theory of hidden crossings. The main idea is that one electron (or more) molecular orbital(s) is promoted into the continuum carrying with it the symmetry character of that promoted orbital. This character is then revealed in the form of the continuum velocity distribution. According to their explanation, two series of transitions can contribute to the saddle-point ionization mechanism. The T00 series involves no angular momentum transfer and thus leads to a maximum on the

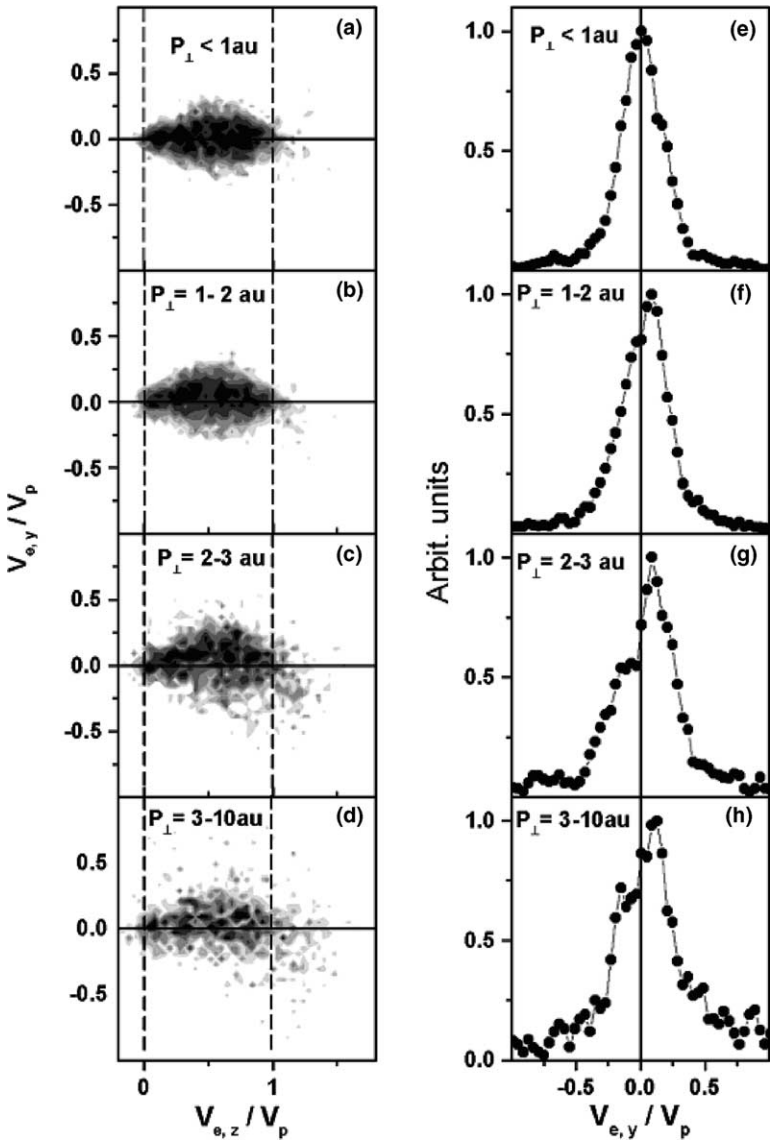

Fig. 4. (a)–(d) Top view of the ejected electron distribution in the collision 0.78 a.u. p on H_2, leading to the single ionization of H_2, for different windows on the magnitude of the transverse momentum transfer ($P_\perp$). (e)–(h) Vertical slices from (a) to (d) projected onto the $V_{e,y}/V_p$ axis for $0.4 < V_{e,z}/V_p < 0.6$.

saddle (σ state). The T01 series originates from rotational coupling between the $2p\sigma$ and the $2p\pi$ states at small internuclear distance leading to a node on the saddle (π state). It is also interesting to note, that as the recoil-ion transverse momentum becomes larger, the tendency for the electrons to follow the scattered projectile in the transverse direction (+y-axis) and to scatter away from the recoil ion and toward the scattered projectile increases (see Fig. 4).

Electron velocity distributions emitted in the TI of H_2 (reaction 2) for side and top views are given in Fig. 5(a) and (b). Two groups of electrons with different structures are clearly visible in these dis-

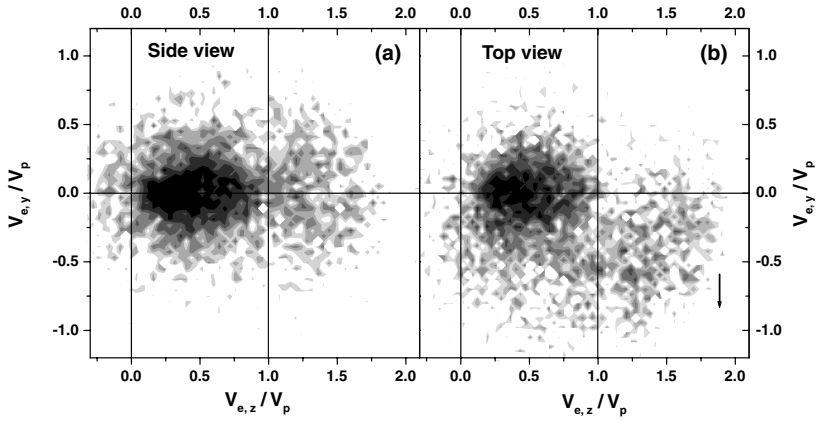

Fig. 5. (a) Side view and (b) top view of the ejected electron velocity distribution in the collision $V_p = 0.78$ a.u. p on H_2 leading to H_2 dissociation into two free protons ($p + H_2 \rightarrow H + H^+ + H^+ + e^-$). The intensity of each cell is proportional to the number of counts in that cell. Each image has been normalized so its maximum intensity is near ten units on this scale. The electron velocity components $V_{e,y}$ and $V_{e,z}$ are scaled by the projectile velocity. The arrow in (b) points to the direction of the recoil.

tributions. The first group consists of electrons emitted in the forward direction with velocities between zero and V_p; the saddle electrons. The other group consists of electrons ejected with velocity greater than the projectile velocity. This group is referred to as the fast forward electrons [22]. Similar behavior has been seen in the experimental work of Moshammer et al. [24] on the single ionization of He at high impact energies. A peak is centered around an electron velocity which is approximately twice that of the projectile ($V_{e,z} \approx 2V_p$) known as the "*binary-encounter*" peak. This peak has been interpreted as a two-body ionization involving momentum exchange between projectile and electron. In the collision system under study, typical electron momenta in the transverse direction are one order of magnitude smaller than the transverse momentum exchange between the heavy particles. Furthermore, the fast forward electrons are mainly centered around $V_{e,z} \approx 1.25V_p$ in the velocity space as shown in Fig. 5. Thus the arguments of "binary-encounter" ionization mechanism which work at high impact energies do not apply at low energies.

The top-view (see Fig. 5(b)) shows that the saddle electrons are concentrated on the internuclear axis. This structure can be seen more clearly by making a transverse projection of the two-dimensional distribution onto the y-axis ($V_{e,y}$) as shown in Fig. 6(b). This is a clear signature of a promotion mechanism via σ states, i.e. via the T00 series, which involves no angular momentum transfer. To demonstrate the dependence of this structure on the impact parameter, the top-view electron velocity distribution was gated on different ranges of transverse momentum transfer, i.e. for different ranges of impact parameters. The results are presented in Fig. 7(a) and (b). These figures reveal that the σ-state is dominant over all ranges of the transverse momentum transfer (i.e. over all ranges of impact parameter). The fast forward electrons possess a different structure than the saddle point electrons. These electrons reveal a substantial amount of out-of-plane scattering as shown in the side-view distribution; Fig. 5(a). The top-view distribution (Fig. 5(b)) shows that the fast forward electrons are emitted opposite to the scattered projectile. To further explore these fast forward electrons, the two-dimensional electron velocity distribution in Fig. 5(b) is projected onto the beam axis ($V_{e,z}$). The projection is given in Fig. 6(a). This figure shows that the fast forward electrons form a peak and yield a significant contribution to the transfer ionization cross section. An obvious indication of the existence of the fast forward electrons could be seen in the theoretical work of Sidky et al. [11] Fig. 1 and [12] Fig. 3. They found classically as well as in using their two-center

Fig. 6. (a) and (b) are respectively the Z- and Y-components of the velocity distribution of electrons ejected in the collision $V_p = 0.78$ a.u. p on H_2 leading to H_2 dissociation into two free protons ($p + H_2 \rightarrow H + H^+ + H^+ + e$) for side and top views.

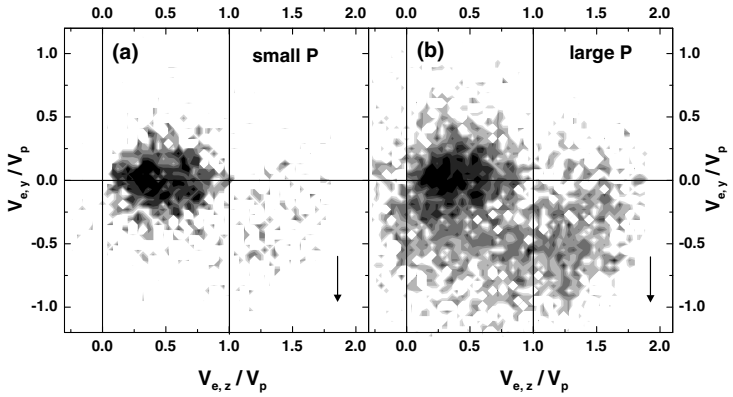

Fig. 7. Top view of the velocity distribution of electrons emitted in the collision 0.78 a.u. p on H_2, leading to H_2 dissociation into two free protons ($p + H_2 \rightarrow H + H^+ + H^+ + e^-$), (a) for small transverse momentum transfer (distant collisions; $P_\perp < 1.5$ a.u.) and (b) for large transverse momentum transfer (close collisions; $P_\perp > 1.5$ a.u.).

momentum space discretization (TCMSD) method [12], a significant emission of fast forward electrons ($V_{e,z} > V_p$). They provided a classification of ejected electrons into saddle electrons and kinetic electrons. This classification is consistent with the results presented in this contribution. Furthermore, this structure has been observed by Ponce et al. [25] in the electron probability density computed by solving the time-dependence Schrödinger equation for the $H^+ + H$ collision system at a projectile velocity of 1 a.u. A maximum in this electron probability density can be seen where the electrons traveling faster than the projectile. However, in the absence of explicit calculations for either total cross sections or emitted electron velocity distributions for collision systems such as the collision system studied in this contribution, no conclusive interpretation of the data can be drawn. The impact parameter study of the electron velocity distribution demonstrates the fact that the emission of the fast forward electrons exhibits a strong impact parameter dependence as shown in Fig. 7(a) and (b). These figures show that the fast forward electrons result from a narrow range of impact parameters. This can be seen more clearly in Fig. 8(a) and (b).

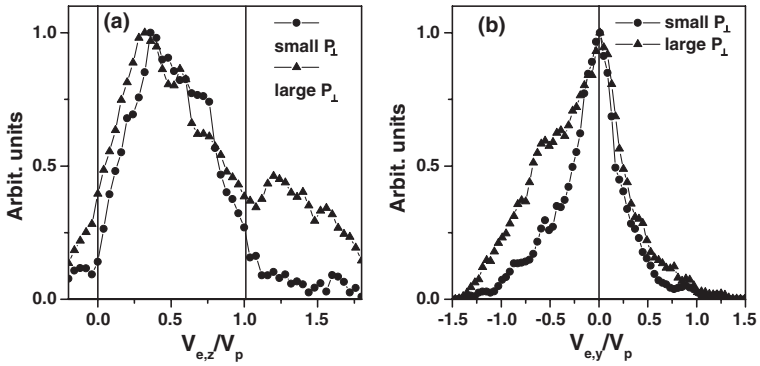

Fig. 8. (a) and (b) are respectively the Z- and Y-components of the velocity of electrons ejected in the collision $V_p = 0.78$ a.u. p on H_2 leading to H_2 dissociation into two free protons ($p + H_2 \rightarrow H + H^+ + H^+ + e$) for small and large ranges of transverse momentum transfer (i.e. distant and close collisions). The arrows in both figures point to the direction of the recoil.

4. Conclusion

Using the COLTRIMS technique, velocity-space images of the electron continua produced by 15 keV protons on H_2 were obtained for a fully determined motion of the nuclei. The spectra show clear qualitative differences between ionizing cases where (a) σ-structure from radial coupling and (b) π-structure where rotational coupling is likely to dominate. The impact-parameter dependence of the electron velocity distributions for single and transfer ionization was also investigated. It is observed, in the case of SI of H_2, that the σ-structure appears in the saddle vicinity for large ranges of impact parameters. However, at small impact parameters, the electron velocity distribution exhibits the nodal line on the saddle (π-structure). The electron velocity distribution for the TI of H_2 unveils the presence of electrons moving faster forward than the projectile. These electrons scatter away from the scattered projectile in the transverse direction. They result from a narrow range of impact parameters (close collisions).

Acknowledgments

F.A. gratefully acknowledges support from the DAAD and the DFG. We thank RoentDek Handels GmbH for the preparation of the position sensitive detectors and other technical equipment. This work is supported by the DAAD, the DFG and the BMBF and the Volkswagen Stiftung.

References

[1] R.E. Olson, Phys. Rev. A 27 (1983) 1871.
[2] R.E. Olson, Phys. Rev. A 33 (1986) 4397.
[3] R.E. Olson, T.J. Gay, H.G. Berry, E.B. Hale, V.B. Irby, Phys. Rev. Lett. 59 (1987) 36.
[4] T.G. Winter, C.D. Lin, Phys. Rev. A 29 (1984) 3071.
[5] T.G. Winter, Phys. Rev. A 37 (1988) 4656.
[6] G. Bandarage, R. Parson, Phys. Rev. A 41 (1990) 5878.
[7] C. Illescas, I. Rabadan, A. Riera, Phys. Rev. A 57 (1998) 1809.
[8] S.Yu. Ovchinnikov, E.A. Solov'ev, Zh. Eksp. Teor. Fiz. 90 (1986) 92, Sov. Phys. JETP 63 (1986) 538; 1989 Comment. At. Mol. Phys. 22 (1988) 69.
[9] M. Pieksma, S.Yu. Ovchinnikov, J. Phys. B 24 (1991) 2699.
[10] S.Yu. Ovchinnikov, J.H. Macek, Phys. Rev. Lett. 75 (1995) 2474.
[11] S.Yu. Ovchinnikov, J.H. Macek, D.B. Khrebtukov, Phys. Rev. A 56 (1997) 2872.
[12] J.H. Macek, S.Yu. Ovchinnikov, Phys. Rev. Lett. 80 (1998) 2298.
[13] R. Dörner, H. Khemliche, M.H. Prior, C.L. Cocke, J.A. Gary, R.E. Olson, V. Mergel, J. Ullrich, H. Schmidt-Böcking, Phys. Rev. Lett. 77 (1996) 4520.
[14] E.Y. Sidky, C. Illescas, C. Lin, Phys. Rev. Lett. 85 (2000) 1634.
[15] E.Y. Sidky, C. Lin, Phys. Rev. A 60 (1999) 377.
[16] R. Dörner, V. Mergel, O. Jagutzki, L. Spielberger, J. Ullrich, R. Moshammer, H. Schmidt-Böcking, Phys. Rep. 330 (2000) 96.

[17] J. Ullrich, R. Moshammer, A. Dorn, R. Dörner, L.Ph.H. Schmidt, H. Schmidt-Bocking, Rep. Prog. Phys. 66 (2003) 1463.
[18] S.D. Kravis et al., Phys. Rev. A 54 (1996) 1394.
[19] M. Abdallah, L.C. Cocke, W. Wolff, H. Wolf, S. Kravis, M. Stöckli, E. Kamber, Phys. Rev. Lett. 81 (1998) 3627.
[20] M. Abdallah, W. Wolff, H.E. Wolf, L.C. Cocke, M. Stöckli, Phys. Rev. A 58 (1998) R3379.
[21] M. Abdallah, W. Wolff, H.E. Wolf, L.C. Cocke, M. Stöckli, J. Phys. B 32 (1999) 4237.
[22] F. Afaneh, R. Dörner, L. Schmidt, Th. Weber, K.E. Stiebing, O. Jagutzki, H. Schmidt-Böcking, J. Phys. B 35 (2002) L229.
[23] L.Ph.H. Schmidt, F. Afaneh, M. Schöller, J. Titze, O. Jagutzki, Th. Weber, K.E. Stiebing, R. Dörner, H. Schmidt-Böcking, Phys. Scrip. T 110 (2004) 379.
[24] R. Moshammer, J. Ullrich, H. Kollmus, W. Schmitt, M. Unverzagt, H. Schmidt-Böcking, C.J. Wood, R.E. Olson, Phys. Rev. A 56 (1997) 1351.
[25] L. Ponce, R. Taïeb, V. Véniard, A. Maquet, J. Phys. B 37 (2004) L297.